L_p-norm minimization for stochastic process power spectrum estimation subject to incomplete data

Yuanjin Zhang [a], Liam Comerford [b,*], Ioannis A. Kougioumtzoglou [c], Michael Beer [a,b,d]

[a] Institute for Risk and Uncertainty, University of Liverpool, Liverpool L69 3GH, UK
[b] Institute for Risk and Reliability, Leibniz University Hannover, Germany
[c] Department of Civil Engineering and Engineering Mechanics, Columbia University, New York, NY 10027, USA
[d] International Joint Research Center for Engineering Reliability and Stochastic Mechanics (ERSM), Tongji University, China

ARTICLE INFO

ABSTRACT

A general L_p norm ($0 < p \leq 1$) minimization approach is proposed for estimating stochastic process power spectra subject to realizations with incomplete/missing data. Specifically, relying on the assumption that the recorded incomplete data exhibit a significant degree of sparsity in a given domain, employing appropriate Fourier and wavelet bases, and focusing on the L_1 and $L_{1/2}$ norms, it is shown that the approach can satisfactorily estimate the spectral content of the underlying process. Further, the accuracy of the approach is significantly enhanced by utilizing an adaptive basis re-weighting scheme. Finally, the effect of the chosen norm on the power spectrum estimation error is investigated, and it is shown that the $L_{1/2}$ norm provides almost always a sparser solution than the L_1 norm. Numerical examples consider several stationary, non-stationary, and multi-dimensional processes for demonstrating the accuracy and robustness of the approach, even in cases of up to 80% missing data.

1. Introduction

Reconstruction of discrete time/space signals that suffer from missing data has long been a topic of interest across a range of fields. Whilst the most effective way to address such problems is to sample signals more reliably, under controlled conditions, this is not always possible. "Missing data" in general, refers to situations in which undesirable gaps occur in data sets. For example, in practice, such problems may be caused by sensor failures or sampling/threshold limitations on the equipment, acquisition or usage restrictions on sensing or on the data itself, and even from data corruption. Re-sampling missing data can be difficult in many cases, and often impossible when working with non-stationary stochastic processes. For this reason, there are numerous approaches to addressing these problems by predicting missing datum values based on the available data. These include zero-padding of missing data [1], least-squares spectral analysis [2–4], iterative spectral de-noising [5–7], interpolative as well as autoregressive methods [8]. Clearly, in most cases the choice of the approach is problem-dependent, and typically depends on a priori known information such as the arrangement and amount of missing data. This paper focuses on a class of missing data problems for which the property of "sparsity" is exploited to reconstruct records. A sparse discrete-time signal can be characterized by a relatively small number of coefficients with respect to its sample length. This sparsity may be apparent in the sampling domain, for which the majority of the data is zero except

for a handful of spikes, or sparsity can occur in some other basis or frame, such as the frequency domain. Signal reconstruction methods that take advantage of sparsity have received increased interest with the advent of Compressive Sensing (CS) [9,10], a signal processing technique in which data are purposely under-sampled.

Regarding applications in structural engineering/dynamics, so far CS has been mostly applied in situations where some saving in data capture time or data size is useful. For example, sensors (especially wireless ones) that capture data for real-time structural health monitoring can be designed to capture only a fraction of the data, reducing manufacturing cost. By utilizing CS with an appropriate compression basis (in which the signal has a sparse representation), data series with far higher resolution than those originally captured could be reconstructed. Not only would the sensors not need to capture as much data, but also the stored data would have a small file size, negating the requirement for compression processing at the sensor. In this regard, some preliminary recent results exist in the literature for structural system parameters identification, damage detection and health monitoring [11–21]. However, most of the aforementioned applications are restricted in the sense that they are focused on the problem of compressing efficiently the acquired signal (assumed to be complete) for circumventing the computational burden of compressing it locally at the sensor. Nevertheless, applying CS theory to the problem of missing data differs primarily in one respect; that is, missing data are not necessarily intentional. Unfortunately, this removes control over one important step of CS: the arrangement of the sampling matrix. CS relies on the choice of an appropriate sampling matrix. For instance, uniform random Fourier matrices obey the CS requirements for sparse reconstruction with high probability [9,10]. Unfortunately, the missing data may not be uniformly distributed over the record; thus, regular or large gaps of missing data can lead to lower orthogonality between random columns of the sampling matrix. Further, even the papers that address the case of data losses such as in [12], focus primarily on deterministic signal reconstruction (e.g. in the time domain). Nevertheless, there are cases (e.g. system reliability assessment applications) where the main objective may not be signal reconstruction (in the time/space domains), but rather characterization and quantification of the underlying stochastic process/field statistics (i.e. Power Spectrum estimation).

Recently, the authors utilized sparse signal reconstruction methods to develop stochastic process power spectrum estimation techniques subject to signals with missing data [22]. The concept of the power spectrum has been indispensable for characterizing stochastic processes that exhibit frequency-dependent properties (e.g., [23–25]). Nevertheless, to estimate the power spectrum of a stochastic process, recorded realizations are often required, which may suffer from previously mentioned missing data problems. Note that power spectrum estimation methods that rely on the Discrete Fourier Transform (DFT) or on wavelet transforms for the non-stationary case, require full, uniformly sampled data sequences; hence the need for reconstruction. In this regard, many processes for which a power spectral model is of interest exhibit relative sparsity in the frequency domain, and thus, sparse reconstruction methods can be ideal. In [26], a CS based approach was developed for power spectrum estimation, in which multiple records were utilized to iteratively update a harmonic basis matrix, demonstrating significantly improved results over alternative methods, and has been applied in the context of structural response and reliability analysis [27]. Further, it is noted that for both stationary and non-stationary processes for which only single records are available, windowing and down-sampling may be applied to emulate multiple process records.

In the above contributions [26,27], L_1 norm minimization was utilized for signal reconstruction, which is commonly applied within a CS framework. In this paper, the power spectrum is estimated by utilizing an alternative $L_{1/2}$ norm minimization procedure. This is more likely to lead to sparser signal reconstruction, with enhanced accuracy. Set within the aforementioned iterative scheme [26], and assuming that multiple process records are available for analysis, $L_{1/2}$ norm minimization solutions are presented alongside L_1, demonstrating the effect of enhanced sparsity upon the "mean" spectrum. It is important to note, however, that there exist several alternative reconstruction schemes in the literature that make use of the L_p $(0 < p \leq 1)$ norm [28], or approach the problem from a probabilistic perspective such as Bayesian compressive sensing (BCS) [29,30]. The latter is able to provide a measure of noise present in the record and estimate the error in the reconstruction. In this regard, BCS may present an ideal tool for use in conjunction with the iterative basis re-weighting utilized herein, where the relationship between error in the individual reconstruction vs the error in the ensemble estimated spectrum is of prime interest.

The following section comprises a brief background to identification of sparse solutions via L_p norm $(0 < p \leq 1)$ minimization schemes. Further, it provides an overview of the L_1 norm re-weighting procedure that utilizes multiple stochastic process records for power spectrum estimation described in detail in [26]. The re-weighting procedure is then utilized alongside $L_{1/2}$ norm minimization, further promoting sparsity. Both methods are then compared for varying numbers of available process records for stationary, non-stationary and multi-dimensional cases.

2. Sparse solutions via L_p norm minimization

The condition of sparsity requires that a signal can be defined in some known basis with far fewer coefficients than the number determined by the Shannon-Nyquist rate [31]. As an example, a discrete time signal x in one dimension can be viewed as an $N \times 1$ column vector. Given an orthogonal $N \times N$ basis matrix A, in which the columns A_i are the basis functions, x can be represented in terms of this basis via a set of $N \times 1$ coefficients y, i.e.,

$$x = \sum_{i=1}^{N} A_i y_i, \tag{1}$$

The vector x is said to be K-sparse in the basis A if y has K non-zero entries and $K < N$, i.e.,

$$x = \sum_{i=1}^{K} A_{n_i} y_{n_i}, \tag{2}$$

where n_i are the integer locations of the K non-zero entries in y. Hence y is an $N \times 1$ column vector with only K non-zero elements. Therefore,

$$|y|_{L_0} = K, \tag{3}$$

where L_0 is a 'pseudo' norm defined as the number of non-zero entries in the vector y, i.e.,

$$|y|_{L_0} = \sum_i |y_i|^0. \tag{4}$$

Further, for $p > 0, |.|_{L_p}$ denotes the L_p norm defined as

$$|y|_{L_p} = \left(\sum_i |y_i|^p \right)^{\frac{1}{p}}. \tag{5}$$

Considering an under-sampled signal, transformation into a new basis (e.g., Fourier, wavelets etc) leads to an under-determined system of equations, i.e.,

$$x = By \tag{6}$$

where B is an $M \times N$ reduced A matrix where $M < N$. The assumption that a signal is uniquely sparse in the given basis provides an objective to solving these equations. In general, if a unique sparsest solution of an under-determined system of equations exists, it is found when the L_0 norm is minimized. According to [32], this L_0 solution is said to be the exact reconstruction of the original signal with high probability if $M > CK \log(N)$ for some constant C, where as C increases, so does the probability of successful reconstruction. This L_0 optimization problem is non-convex with no known exact solution [9,33]. However, a viable alternative exists in minimizing the L_1 norm instead. L_1 norm minimization promotes sparsity and in many cases will yield the same result as L_0 norm minimization [34]. Further, the problem becomes convex, and may be set in a convenient linear programming form, i.e.

$$\min |y|_{L_1} \ subject \ to \ x = By \tag{7}$$

Eq. (7) describes a basis pursuit optimization problem and can be easily solved via a gradient-based method, e.g. [35]. This notable feature led some of the authors to applying L_1 minimization in a CS framework for estimating the relatively narrow-band (evolutionary) power spectra of stationary and non-stationary stochastic processes based on available realizations with incomplete data [22,26]. However, as minimizing the L_1 norm does not guarantee the sparsest solution, reconstruction can be improved, or accurately met with fewer sample data, when utilizing L_p norm minimization with $p < 1$. Although such problems appear to be non-convex, it was shown in [36] that even when finding a local minimum, exact reconstruction is possible with far fewer data than those required for L_1 reconstruction.

In fact, it was shown in [37] that $p = 1/2$ tends to yield the sparsest solution for $1/2 \leqslant p < 1$ and for $0 < p < 1/2$ the sparsity degree remains relatively unaffected. Hence, in this paper, $L_{1/2}$ norm minimization is considered to be representative of the $p < 1$ cases for reconstruction of sparse signals. The herein utilized scheme for implementing the $L_{1/2}$ norm is based upon on a re-weighted least squares algorithm [36,38]. In this regard, the L_1 minimization problem in Eq. (7) becomes

$$\min |y|_{L_{1/2}} \ subject \ to \ x = By. \tag{8}$$

To minimize Eq. (8), the Lagrangian $L(y, \lambda)$ is introduced as

$$L(y, \lambda) = \sum_n |y_i|^{\frac{1}{2}} + \lambda^T (By - x). \tag{9}$$

The partial derivatives of Eq. (9) with respect to y and λ are equal to zero when

$$y = QB'(BQB')^{-1} x, \tag{10}$$

for $Q = \text{diag}(|y|^{\frac{2}{3}})$. Eq. (10) can be solved iteratively by computing Q from the solution of each previous iteration, i.e.,

$$y_k = Q_{k-1} B'(BQ_{k-1}B')^{-1} x, \tag{11}$$

$$Q_{k-1} = \text{diag}\left(|y_{k-1}|^{\frac{2}{3}} \right). \tag{12}$$

Note that this algorithm is equivalent to a weighted L_2 norm [38]

$$\min_{y} \sum w_i y_i^2 \text{ subject to } x = By \tag{13}$$

where $w_i = |y_{i,k-1}|^{-3/2}$. As the solution is sparse, the value of many y_i will tend toward zero. To avoid division by zero in w_i as the algorithm converges to a solution, a decreasing parameter ϵ is introduced to regularize the optimization problem [39], i.e.,

$$Q_{k-1} = \text{diag}\left(\left(|y_{k-1}|^2 + \epsilon_j \cdot \text{mean}(|y_{k-1}|^2) \right)^{\frac{3}{4}} \right), \tag{14}$$

$$\epsilon_j = \frac{\epsilon_{j-1}}{10}, \tag{15}$$

where $\epsilon_0 = 1$ and for each ϵ_j Eq. (11) is repeated until satisfying

$$\frac{\|y_k - y_{k-1}\|_2}{\|y_{k-1}\|_2} < \frac{\sqrt{\epsilon_j}}{100} \tag{16}$$

Converging to the true $L_{1/2}$ solution can largely depend upon the initialization of Q. Fortunately, in the case where multiple process records are used to estimate the power spectrum (a core assumption of the adaptive basis method presented in the next section), a satisfactory approximation of y can be realized on which to initialize the $L_{1/2}$ norm minimization algorithm. Essentially any standard spectrum estimation method that can process "gappy" records, such as least-squares (L_2 norm), can be used to produce an average estimation of the power spectrum across the ensemble, yielding suitable initialization coefficients for Q. The proposed initialization of Q for both stationary and non-stationary cases is based on a least squares estimation of y. Note that when utilizing multiple records, this initial estimation may also take advantage of the re-weighting procedure detailed in Section 4.

Naturally, recorded signals are rarely ever truly sparse; even low levels of measurement noise will produce small coefficients across most bases. Further, particularly for power spectra that describe environmental processes, even without noise, they may inhabit the entirety of the detectable frequency domain. In these cases the smallest coefficients may be assumed to be equal to zero, with the focus placed on detecting the size and location of the dominant spectral peaks. To account for both noise and negligible coefficients, a tolerance, e, is included. Thus, Eqs. (7) and (8) are re-cast in the form,

$$\min |y|_{L_p} \text{ subject to } |By - x|_{L_2} \leqslant e. \tag{17}$$

The chosen value of e presents a trade-off between sparsity and accuracy. For the cases where either the signal is not sparse enough or the missing data are too extensive for L_p ($0 < p \leq 1$) minimization to exactly reconstruct the original signal, it is important to note that there may still be significant advantages over a minimum L_2 solution. In spectral estimation, minimizing the L_2 norm (similar to zero-padding) is likely to spread the solution over many frequencies; this is because individually, large coefficients are heavily penalized. Minimizing the L_p ($0 < p \leq 1$) norm however is far more likely to yield larger individual coefficients, having the effect of producing sharp, well-defined peaks at the key frequencies.

3. Stochastic process representation & spectral estimation

To utilize bases in which signals are assumed to be sparse in the context of power spectrum estimation, a mapping is required between the chosen basis, and a power spectrum model. Appropriate basis functions to be used in the context of the previous section are outlined here for both stationary and non-stationary stochastic processes.

3.1. Stationary case

Starting with a stationary model of a real-valued stochastic process, its power spectrum may be given as the ensemble average of the square of the Fourier transform amplitudes of available discrete time realizations [40]; that is,

$$S_X(\omega_k) = \frac{2\Delta T}{T} E \left| \sum_{t=0}^{T-1} X_t e^{-2\pi i k t / T} \right|^2 \tag{18}$$

where T is the number of data points, t is the data point index in the record, ΔT is the sampling time increment, and k is the integer frequency for ω_k (i.e. $\omega_k = \frac{2\pi k}{T_0}$ where T_0 is the total length in time of the record). Hence, the Fourier basis functions are utilized in this case.

3.2. Non-stationary case

A reliable spectral model providing frequency dependent information can be of significant importance in investigating the response of an engineering system to stochastic input. However, a time-invariant spectral model can only describe a stationary process, i.e. one in which the spectral content does not change over time. This assumption of stationarity often produces

a poor approximation of the true process, as many important processes of interest are non-stationary in nature. For example, the frequency content of an earthquake induced excitation can change significantly over its duration, whereas wind systems may contain short infrequent bursts that do not conform to the otherwise stationarity of the rest of the process. Hence, in many cases, accounting for time-dependent properties of stochastic processes is critical in defining reliable spectral models [41,42]. For these reasons, evolutionary power spectrum estimation of non-stationary processes will receive particular attention in the ensuing analysis.

For the case of non-stationary stochastic processes a time/frequency-localized wavelet basis, as opposed to the Fourier decomposition of the signal is utilized. In this regard, Nason et al. [43] developed the wavelet based representation,

$$X(t) = \sum_j \sum_k w_{j,k}\psi_{j,k}(t)\xi_{j,k},$$
(19)

where $\psi_{j,k}(t)$ is the chosen family of wavelets and j and k represent the different scales and translation levels respectively; $\xi_{j,k}$ is a stochastic orthonormal increment sequence. This wavelet-based model relies on the theory of locally stationary processes (see [44]). Next, by utilizing the generalized harmonic wavelets [45,46], defined in the time domain as,

$$\psi_{(m-n),k}(t) = \frac{e^{(in\Delta\omega(t-k))} - e^{(im\Delta\omega(t-k))}}{i(n-m)\Delta\omega(t-k)},$$
(20)

Eq. (19) becomes

$$X(t) = \sum_{(m,n)} \sum_k \left(\sqrt{S^X_{(m,n),k}(n-m)\Delta\omega} \psi_{(m,n),k}(t)\xi_{(m,n),k} \right).$$
(21)

Eq. (21) represents a localized process at scale (m,n) and translation (k) defined in the intervals $[m\Delta\omega, n\Delta\omega]$ and $\left[\frac{kT_0}{n-m}, \frac{(k+1)T_0}{n-m} \right]$, with $S^X_{(m,n),k}$ representing the spectrum $S_X(\omega,t)$ at scale (m,n) and translation (k); see also [47].

Regarding the problem of estimating the EPS of a non-stationary stochastic process based on available/measured realizations, a wavelet process based compatible estimation approach advocates that the EPS $S_X(\omega,t)$ of the process $X(t)$ is estimated by [48,47]

$$S_X(\omega,t) = S^X_{(m,n),k} = \frac{E\left(\left| W^G_{(m,n),k}[X] \right|^2 \right)}{(n-m)\Delta\omega}, \quad m\Delta\omega \leqslant \omega \leqslant n\Delta\omega, \quad \frac{kT_0}{n-m} \leqslant t \leqslant \frac{(k+1)T_0}{n-m},$$
(22)

where $W_{(m,n),k}$ is the generalized harmonic wavelet transform (GHWT) defined as

$$W^G_{(m,n),k} = \frac{n-m}{kT_0} \int_{-\infty}^{\infty} f(t)\overline{\psi_{(m,n),k}(t)}dt.$$
(23)

Thus, the EPS can be estimated as the ensemble average of the square of the wavelet coefficients, whereas the wavelets of Eq. (20) serve as the basis functions.

4. Adaptive basis re-weighting

The adaptive basis re-weighting procedure, first proposed in [26], has been shown to improve the stochastic process power spectrum estimate to a large extent. The rationale relates to exploiting the presence of the expectation operators in Eqs. (18) and (22) for estimating power spectra. Given multiple process records, the objective is to estimate the power spectrum based on the mean square of their transform coefficients. This requires the core assumption that the individual records are produced by the same underlying stochastic process, and thus, are compatible with the same power spectrum. In this case, we would expect the individual record transforms to exhibit similarities. For instance, if the spectral power is estimated to be high at a specific frequency, then each individual record is more likely to have higher amplitude Fourier coefficients at that same frequency. When dealing with missing data, we can use this fact to skew the reconstruction optimization problem in the direction of the ensemble estimated power spectrum, in a similar way to the $L_{1/2}$ minimization presented previously.

The purpose of the re-weighting procedure is to iteratively update a weight matrix W to be used in a least squares optimization, as was the case with Q in Eq. (12). However, rather than base W solely on the outcome of the least squares result, it is based on an ensemble mean. Once the iterations are complete, the final W is multiplied by the basis matrix to influence the result of the chosen L_p norm minimization. Hence, Eqs. (7) and (8) become:

$$\min |y|_{L_p} \text{ subject to } x = WBy$$
(24)

The contribution of a single process record to the next iteration of the re-weighting matrix W_k is given by

$$y_{r,k} = (BW_{k-1})'(BW_{k-1}(BW_{k-1})')^{-1}x,$$
(25)

where B is the reduced $M \times N$ matrix as in Eq. (6) and $y_{r,k}$ is an $N \times 1$ least squares estimation of the rth signal realization's basis coefficients, subject to the $(k-1)^{\text{th}}$ re-weighted basis matrix W_{k-1}. Further, odd and even functions (e.g., sine and cosine) are paired when forming the W matrix and their combined magnitude is used for both individual weights. This is a necessary step as the power spectrum models given by Eqs. (18) and (22) do not exhibit phase-dependent properties. For basis matrices composed of real functions, with odd and even functions of equal frequency adjacent to one another, the W matrix is constructed in the following way:

$$W_k = \text{diag}(w_{k,j=0,1\ldots N}),\tag{26}$$

where

$$w_{k,j} = \frac{\sum_R \left(\sqrt{y_{r,k,j_f}^2 + y_{r,k,j_f+1}^2}\right)}{R} + c.\tag{27}$$

y_{r,k,j_f} are the scalar coefficients at positions j_f from the vector $y_{r,k}$, where,

$$j_f = \text{floor}(j/2),\tag{28}$$

where floor(.) maps a real number to the largest previous integer. In Eq. (27), R is the total number of process realizations in the ensemble, and c is a constant: Although in the case where absolute sparsity is inferred, it might be beneficial to allow weight coefficients to reduce to zero, this assumption is seldom true when dealing with real recorded processes. Therefore, to prevent weight coefficients approaching zero and forcing functions out of the optimization, a constant, positive bias is included. In the following numerical examples, this is set equal to the mean weight at each iteration.

The optimization is initialized with an $N \times N$ identity matrix (i.e., without weights). The procedure is terminated when the change in weights between iterations is considered to be very small,

$$\frac{||W_k - W_{k-1}||_2}{||W_{k-1}||_2} < \delta_W,\tag{29}$$

where δ_w is some small value, several orders of magnitude lower than the mean square of W.

5. Numerical examples

The numerical examples are split into four parts. First, the ability of L_1 and $L_{1/2}$ norm minimization in estimating spectra are compared for a stationary sea wave process without utilizing the basis re-weighting procedure. This first example demonstrates the ability of the $L_{1/2}$ norm minimization in finding sparser solutions. For the remaining parts, the iterative re-weighting procedure is introduced and implemented in both L_1 and $L_{1/2}$ norm minimization procedures over three separate examples, considering stationary sea wave, non-stationary wind and two dimensional material property processes. For each of re-weighting examples, the reconstruction capabilities of L_1 and $L_{1/2}$ norms are assessed utilizing two different sizes of record ensemble; that is, 20 process records and 200 process records. Throughout, for selected examples, estimated spectra utilizing scaled zero-padding are also provided as a baseline comparison. In this case the missing data are replaced with zeros, the appropriate transform is performed, and then scaled relative to the number of missing data.

To assess the reconstruction efficacy in the above scenarios, time histories compatible with pre-defined power spectra are generated. These are produced via the techniques described in [23,42] for stationary and non-stationary processes, respectively. The rationale is that in many cases, ensembles of records from similar wind, sea wave or material properties processes (as in the examples) share similar second-order statistics, and so a mean estimate provides a useful model for each process as a whole. Specifically, for a stationary record, a power spectrum compatible realization is given by,

$$X(t) = \sum_{j=0}^{N-1} \sqrt{4S_X(\omega_j)\Delta\omega} \sin\left(\omega_j t + \Phi_j\right)\tag{30}$$

where Φ_j are uniformly distributed random phase angles in the range $0 \leqslant \Phi_j < 2\pi$ and N relates to the discretization of the frequency domain. For non-stationary processes, $S_X(\omega_j)$ in Eq. (30) is replaced with an evolutionary power spectrum $S_X(\omega_j, t)$.

Next, missing data are imposed to the simulated power spectrum compatible realizations. In the following examples, missing data are considered to occur at random locations drawn from a uniform distribution of the time index i.e.,

$$x_0(t) = \begin{cases} x(t), & \rho \geqslant m \\ 0, & \rho(t) < m \end{cases}\tag{31}$$

where $x_0(t)$ is the realization with missing data, $x(t)$ is the original realization, ρ is a vector of N_0 equally spaced numbers from 0 to 1 arranged in random order, and m is the fraction of missing data. For each sample, new random missing data are generated. The number of missing data in each sample is kept constant for consistency. For real data suffering gaps in this manner, it is possible that different records would contain different numbers of missing data. In this case, the re-weighting procedure is still applicable. Further, it is proposed that each individual record's contribution to the re-

weighting matrix W could be penalized, proportional to the number of missing data. In [22] it was found that power spectrum estimation of stationary processes is relatively insensitive to long gaps in time series, but can have a significant negative impact on non-stationary process spectrum estimation due to the increased coherence between the sampling and basis matrices when utilizing wavelets. This is particularly apparent if the gaps appear in the same location throughout the ensemble. However, such configurations of missing data are not considered in this work.

Note that as the amount of missing data increases beyond the maximum required for exact reconstruction in L_1 or $L_{1/2}$, the number of basis coefficients produced by CS will decrease. For all of the examples herein, the number of missing data imposed renders exact reconstruction of any given record highly unlikely under L_1 or $L_{1/2}$ norm minimization. However, these schemes are ideal for identifying dominant spectral characteristics as opposed to L_p ($p > 1$) norm minimization which penalize high powers in the spectrum (in particular, widely applied zero-padding solutions akin to L_2 norm minimization). When combined across a record ensemble, this information is ideal for "mean" power spectrum estimation, particularly when utilizing the basis re-weighting scheme.

Power spectra may be estimated based on complete realizations of Eq. (30) using the methods outlined in Section 3. They are then compared against those estimated from realizations with simulated missing data. Specifically, a normalized power spectrum error is calculated for stationary processes:

$$error = \frac{\int_0^{\omega_u} |S_E(\omega) - S_T(\omega)|d\omega}{\int_0^{\omega_u} |S_T(\omega)|d\omega}, \tag{32}$$

and for non-stationary processes:

$$error = \frac{\int_0^{\omega_u} \int_0^{t_u} |S_E(\omega, t) - S_T(\omega, t)|d\omega dt}{\int_0^{\omega_u} \int_0^{t_u} |S_T(\omega, t)|d\omega dt}, \tag{33}$$

It is important to note that the error is calculated from two spectral estimates (with missing data and without missing data), and does not utilize the original power spectrum. This is because the objective of this work is not to assess the accuracy of the underlying spectrum estimation method (in this case Fourier or GHW based methods which have already been studied extensively in this context [48–50]), but to investigate, specifically, the effect of the missing data upon spectral estimation. Further, due to the random nature of the generated process records and arrangement of missing data, the calculated error is a random variable for any given case. Hence, statistics are determined for the error as well, by considering an ensemble of power spectrum estimates obtained via repetitions of the same experiment.

5.1. Stationary sea wave spectrum without re-weighting

As previously mentioned, the first example is presented without utilizing the basis re-weighting procedure to demonstrate the un-biased difference between L_1 and $L_{1/2}$ solutions. The fact that $L_{1/2}$ is shown to out-perform L_1 indicates that it could be a more appropriate choice when estimating spectra from single process records (where the basis re-weighting procedure may not be applicable). Note that in this example, Q in Eq. (11) is initialized using a least squares estimation of y,

$$Q_0 = \text{diag}(q_0), \tag{34}$$

where

$$q_0 = B'(BB')^{-1}x. \tag{35}$$

In Eq. (35) B is the reduced $M \times N$ basis matrix and x is the time-history record after data have been removed. The JONSWAP sea wave spectrum of Eq. (36) [51] is used to produce stationary process time histories,

$$S(\omega) = \frac{ag^2}{\omega^5} e^{(5/4)\left(\omega_\rho/\omega\right)^4} \gamma^r; r = e^{-\left((\omega - \omega_\rho)/2\sigma\omega_\rho\right)^2}, \tag{36}$$

where $\alpha = 0.03, \omega_\rho = 0.05, \gamma = 3.3$ and, $\sigma = \begin{cases} 0.07, & \omega < \omega_\rho \\ 0.09, & \omega > \omega_\rho \end{cases}$. Figs. 1 and 2 show the target spectra along with the reconstructed spectra for L_1 norm and $L_{1/2}$ norm minimization averaged over 20 samples and 200 samples, respectively. For these examples, spectra were reconstructed after 75% of the data were removed via Eq. (31). While in both figures, the L_1 and $L_{1/2}$ norms succeed in determining spectra that match moderately well with the target, a trend emerges when comparing the calculated errors for spectral estimates produced from 20 and 200 samples, which are shown as normalized histograms in Fig. 3. Note that for all four cases (L_1 and $L_{1/2}$ norm with 20 and 200 samples), the results were repeated 500 times to produce these histograms due to the fact that any single error result is not representative of the full set. In both cases, the $L_{1/2}$ solution leads to spectral estimates with lower error than the L_1 solution. However, it is clear from Fig. 3 that this difference becomes more prominent as the number of samples increases. It should also be noted that even for the 20 sample case (in which the histograms intersect), for each sample set, the $L_{1/2}$ norm solution produced a lower error than the L_1 norm solution.
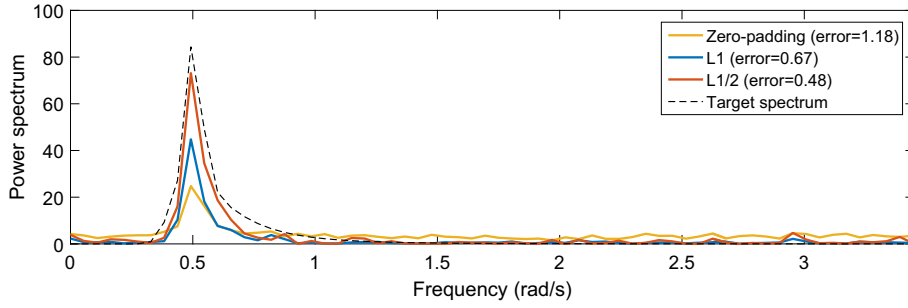
Fig. 1. JONSWAP stationary power spectrum estimates of Eq. (36) from 20 samples without re-weighting (75% missing data).
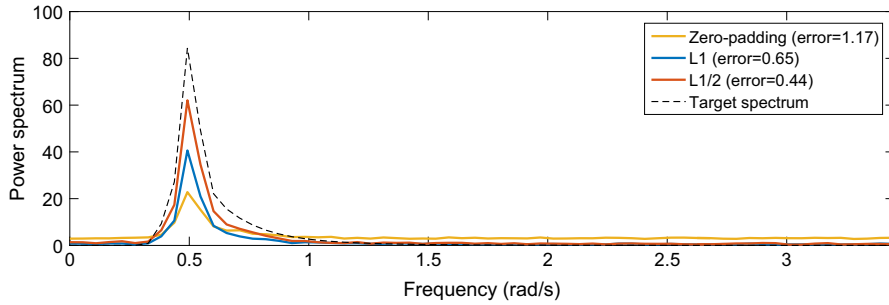

Fig. 2. JONSWAP Stationary power spectrum estimates of Eq. (36) from 200 samples without re-weighting (75% missing data).
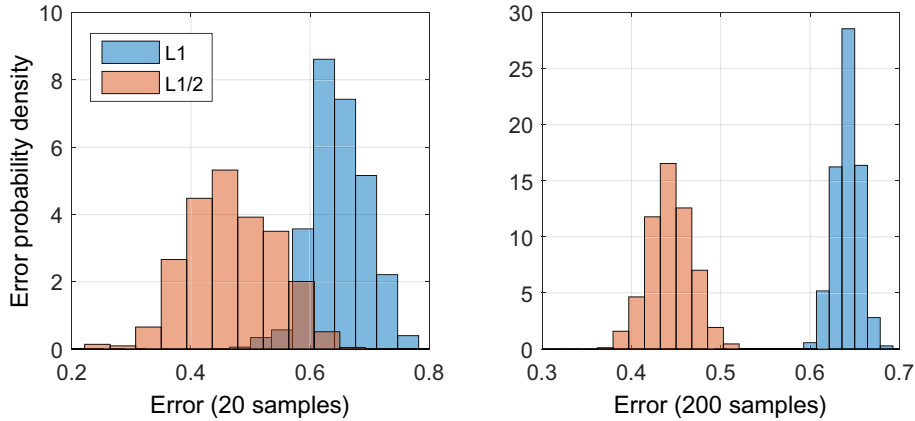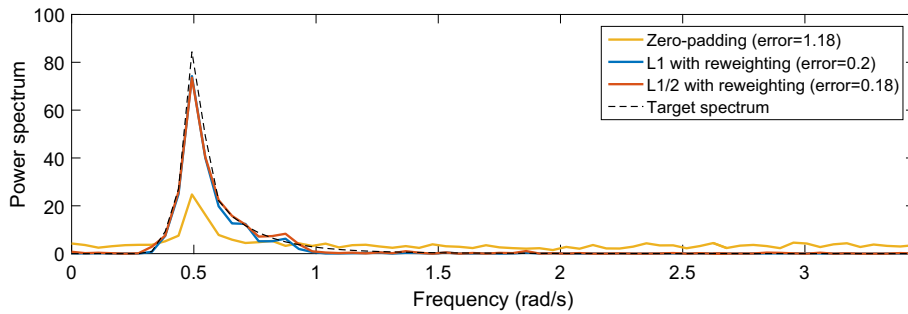

Fig. 3. Distribution of error over 500 repeated estimations of Eq. (36) without re-weighting for 20 and 200 samples.

5.2. Stationary sea wave spectrum with basis re-weighting

The following example is similar to the previous one, with the exception that when solving the L_p norm minimization problems, the weighted Fourier basis is used instead of the original orthonormal one. The same weight matrix is used for both L_1 and $L_{1/2}$ norm problems, calculated again, based on 20 and 200 process records. For the $L_{1/2}$ norm minimization algorithm, Q is this time initialized after taking account of the final weight matrix,

$$Q_0 = \text{diag}(q_0), \tag{37}$$

where

$$q_0 = (WB)'(WB(WB)')^{-1}x. \tag{38}$$

Figs. 4 and 5 show the target spectra along with the reconstructed spectra for L_1 norm and $L_{1/2}$ norm minimization averaged over 20 samples and 200 samples, respectively. Again, 75% of the data were removed based on Eq. (31). The errors with reference to the target spectrum estimates are shown as histograms for 500 test runs in Fig. 6 for 20 and 200 time histories.

Fig. 4. JONSWAP stationary power spectrum estimates of Eq. (36) from 20 samples with re-weighting (75% missing data).
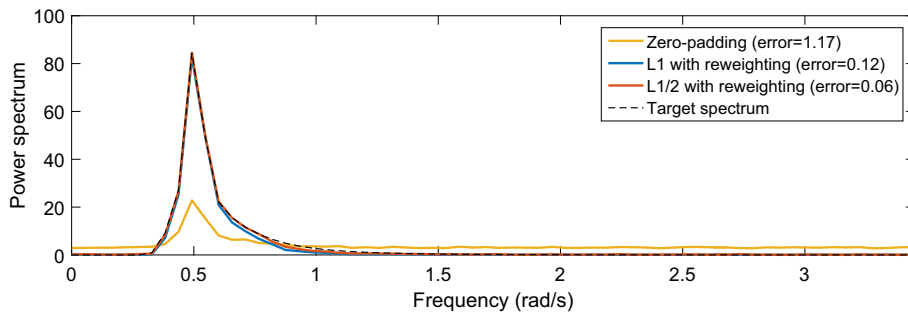

Fig. 5. JONSWAP stationary power spectrum estimates of Eq. (36) from 200 samples with re-weighting (75% missing data).
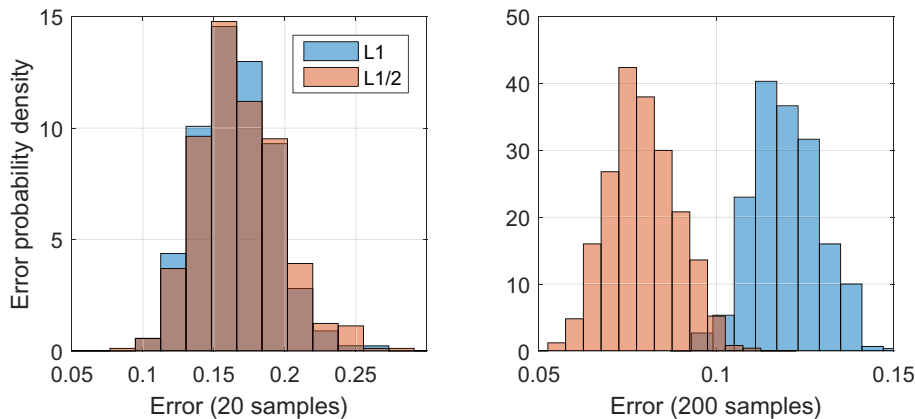

Fig. 6. Distribution of error over 500 repeated estimations of Eq. (36) with re-weighting for 20 and 200 samples.

As with the non re-weighted case, the distribution of error changes with number of samples used to estimate the spectrum. However, when comparing Fig. 6 to Fig. 3, it is clear that the re-weighting procedure has had a significant effect. Firstly, the mean error for both cases has decreased dramatically, this is also apparent when comparing the plotted spectra in the non re-weighted case (Figs. 1 & 2) to the re-weighted case (Figs. 4 & 5). Secondly, the L_1 norm solution has also improved relative to the $L_{1/2}$ solution. In fact, for 20 samples, the L_1 norm solution provided a superior spectral estimate in $> 70\%$ of trials. However, in the 200 sample case, despite the slight overlap in the histograms (Fig. 6, right), for each individual trial, the $L_{1/2}$ norm solution provided the lowest error. Finally a 200 sample case was run with Poisson white noise added to the time-domain signal with variance equal to 10% of the r.m.s of the original to demonstrate that the spectral estimates still converge toward the target, shown in Fig. 7.

5.3. Non-stationary wind spectrum with basis re-weighting

For the non-stationary case, the following time-modulated von Karman gust spectrum model [52] is used to generate process realizations:
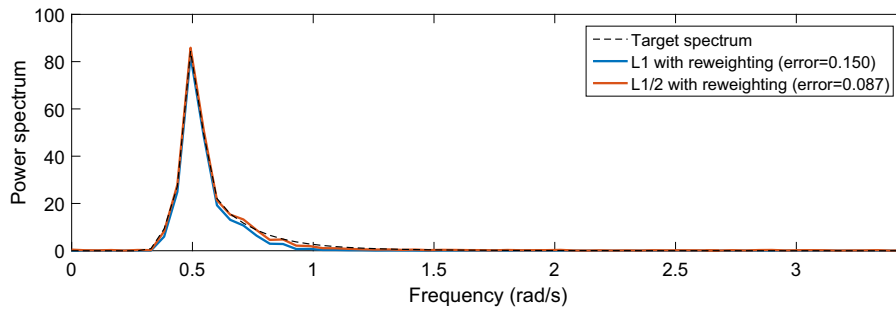
Fig. 7. JONSWAP stationary power spectrum estimates of Eq. (36) with added Poisson noise from 200 samples with re-weighting (75% missing data).

$$S_X(\omega, t) = |g(t)|^2 S_{X0}(\omega),$$ (39)

where

$$g(t) = \sqrt{\alpha_0 t^{\beta_0} e^{-\lambda t}}$$ (40)

and

$$S_{X0}(\omega) = \frac{4\sigma_{X0}^2 L/U}{\left[1 + 70.78\left(\frac{\omega}{2\pi} L/U\right)^2\right]^{5/6}}$$ (41)

where the time modulation parameters are set as $\alpha_0 = 0.0021$, $\beta_0 = 2$, and $\lambda = 0.033$; standard deviation of the stationary process $\sigma_{X0} = 6$, integral length scale $L = 80$, and mean wind speed $U = 40$. The results are produced given the same parameters as the previous stationary case with basis re-weighting, except with a GHW source basis. A wavelet bandwidth of $(n - m = 8)$ is used which offers a satisfactory trade-off between time and frequency resolutions. Figs. 8–11 show the estimated spectrum with no missing data, and with 75% missing data (zero-padded, L_1 and $L_{1/2}$ norm cases), respectively, for 20 realizations only. For ease of comparison, Figs. 12 and 13 show all three estimated spectra compared at a single time instant ($t = 1s$) for both 20 and 200 realizations respectively.

As with the stationary case, the reconstructed spectra compare well with the target with as few as 20 realizations, with a small but noticeable increase in accuracy for 200 realizations. Fig. 14 shows error histograms for the non stationary case. Again, when more samples are used the $L_{1/2}$ norm solution improves compared to the L_1 norm solution (as before, for 200 samples, all of the individual $L_{1/2}$ trials exhibit a lower error), though for the 20 sample case there is almost no difference.

5.4. Two-dimensional stochastic field spectrum with basis re-weighting

Two-dimensional random fields are typically utilized for modelling material properties (e.g. [53]). While the signal of interest is a two-dimensional field, it can be decomposed by rows or columns into a one-dimensional vector. The two-dimensional Fourier decomposition provides a two-dimensional basis matrix for each frequency up to the Nyquist rate.
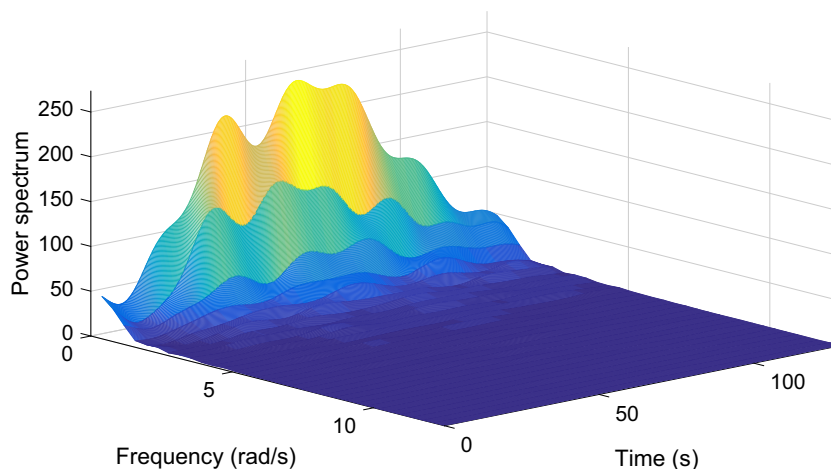

Fig. 8. Evolutionary wind speed power spectrum estimate of Eq. (39) from 20 samples (no missing data).
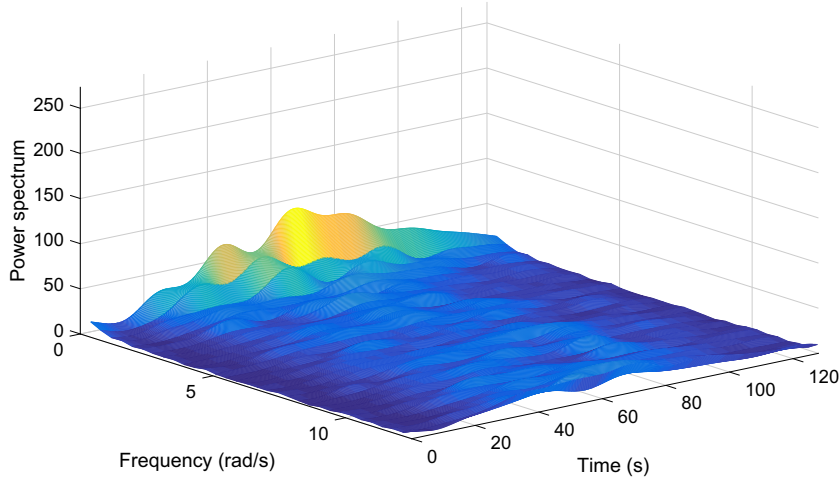
Fig. 9. Evolutionary wind speed power spectrum estimate of Eq. (39) from 20 samples with re-weighting (75% missing data, reconstruction with zero-padding, error = 1.0).
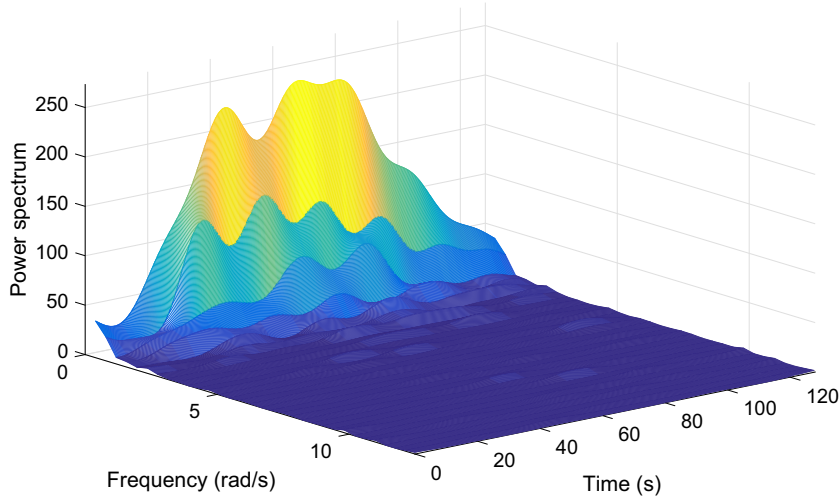

Fig. 10. Evolutionary wind speed power spectrum estimate of Eq. (39) from 20 samples with re-weighting (75% missing data, L_1 norm reconstruction, error = 0.22).

These matrices are also decomposed into one-dimensional vectors to produce a single square basis matrix as in the one-dimensional case. Thus, the problem is treated as in the one-dimensional case.

Further, to generate realizations, a two-dimensional generalization of Eq. (30) is utilized [54], i.e.,

$$g(x_1, x_2) = \sqrt{2} \sum_{n_1}^{N_1-1} \sum_{n_2}^{N_2-1} \left[A_{n_1 n_2} \cos\left(\kappa_{1n_1} x_1 + \kappa_{2n_2} x_2 + \Phi_{n_1 n_2}^{(1)}\right) + \widetilde{A}_{n_1 n_2} \cos\left(\kappa_{1n_1} x_1 + \kappa_{2n_2} x_2 + \Phi_{n_1 n_2}^{(2)}\right) \right] \tag{42}$$

where

$$A_{n_1 n_2} = \sqrt{2 S_g\left(\kappa_{1n_1}, \kappa_{2n_2}\right) \Delta\kappa_1 \Delta\kappa_2}, \tag{43}$$

$$\widetilde{A}_{n_1 n_2} = \sqrt{2 S_g\left(\kappa_{1n_1}, -\kappa_{2n_2}\right) \Delta\kappa_1 \Delta\kappa_2}, \tag{44}$$

and x_j & κ_j are the two-dimensional space and wave number domains respectively.

Note that records generated via Eq. (42) tend to exhibit a Gaussian distribution [54,23], whereas a wide range of techniques exist for producing realizations compatible with a given power spectrum and a non-Gaussian probability density
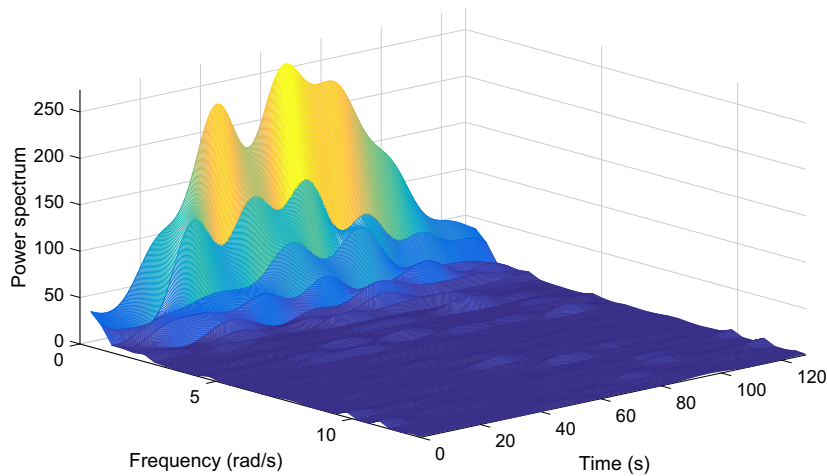
Fig. 11. Evolutionary wind speed power spectrum estimate of Eq. (39) from 20 samples with re-weighting (75% missing data, $L_{1/2}$ norm reconstruction, error = 0.23).
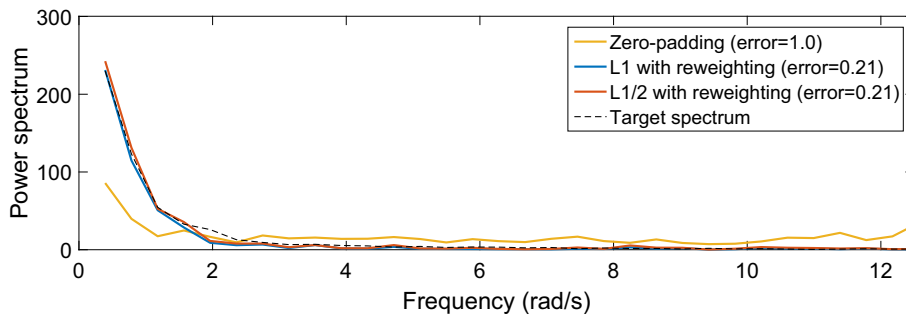

Fig. 12. Evolutionary wind speed power spectrum estimate of Eq. (39) from 20 samples with re-weighting at $t = 70$ s (75% missing data).
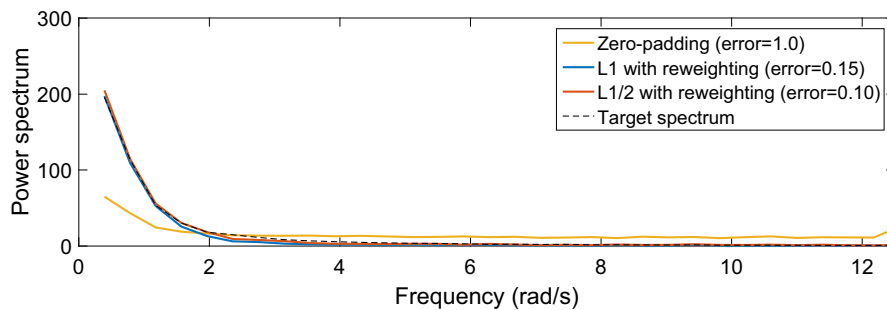

Fig. 13. Evolutionary wind speed power spectrum estimate of Eq. (39) from 200 samples with re-weighting at $t = 70$ s (75% missing data).

function e.g., [55–58]. For instance, following [55], a Gaussian field, denoted by $g(x_1, x_2)$ may be transformed into a non-Gaussian field, $f(x_1, x_2)$ by way of the transformation

$$f(x_1, x_2) = F_f^{-1}(F_g(g(x_1, x_2))), \tag{45}$$

where F_g is the Gaussian cumulative distribution function and F_f^{-1} is the inverse cumulative distribution for the desired non-Gaussian target field $f(x_1, x_2)$.

Next, following [53], the material modulus of elasticity is modelled as a homogeneous stochastic field with a power spectrum and a cumulative distribution function given by

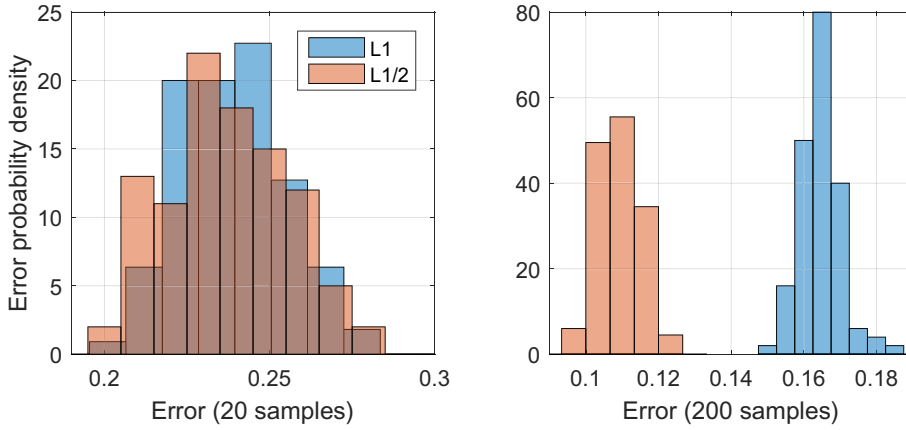$$S(\kappa_1, \kappa_2) = \frac{2}{\pi} \exp(-2(\kappa_1^2 + \kappa_2^2)), \tag{46}$$

Fig. 14. Distribution of error over 100 repeated estimations of Eq. (39) with re-weighting for 20 and 200 samples.
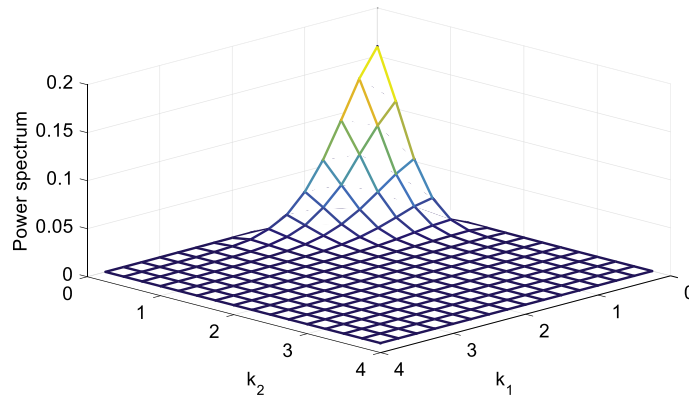

Fig. 15. Two-dimensional non-Gaussian power spectrum estimate of Eq. (46) from 200 samples (no missing data).
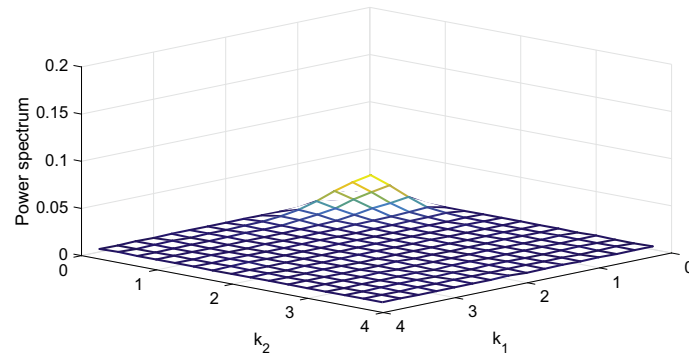

Fig. 16. Two-dimensional non-Gaussian power spectrum estimate of Eq. (46) from 200 samples (80% missing data, reconstruction with zero-padding, error = 1.2).

$$F_f(f(x_1, x_2)) = \frac{f(x_1, x_2) - a_l}{a_u - a_l},$$

(47)

respectively, where $a_u = 0.99$ and $a_l = -0.99$. 80% of the data are removed at uniformly distributed random locations and reconstructed using re-weighted L_1 and $L_{1/2}$ norm minimization for 20 and 200 samples. The target spectrum with no missing data, with zero-padding, and with reconstruction via $L_{1/2}$ norm minimization are shown in Figs. 15–17, respectively (both refer to the 200 samples case). As with the previous examples, histograms showing the distribution of error for repeated tri-
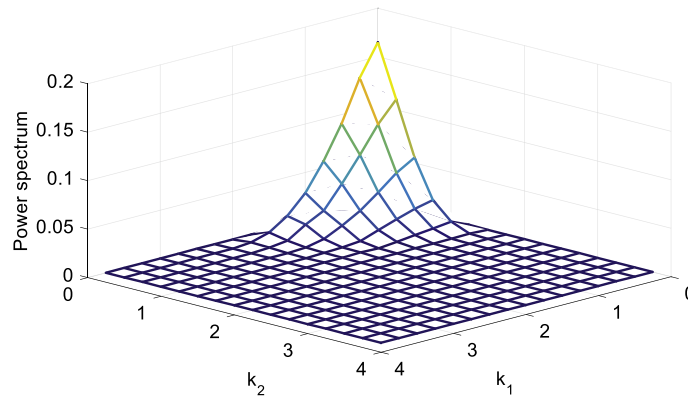
Fig. 17. Two-dimensional non-Gaussian power spectrum estimate of Eq. (46) from 200 samples with re-weighting (80% missing data, $L_{1/2}$ norm reconstruction, error = 0.07).
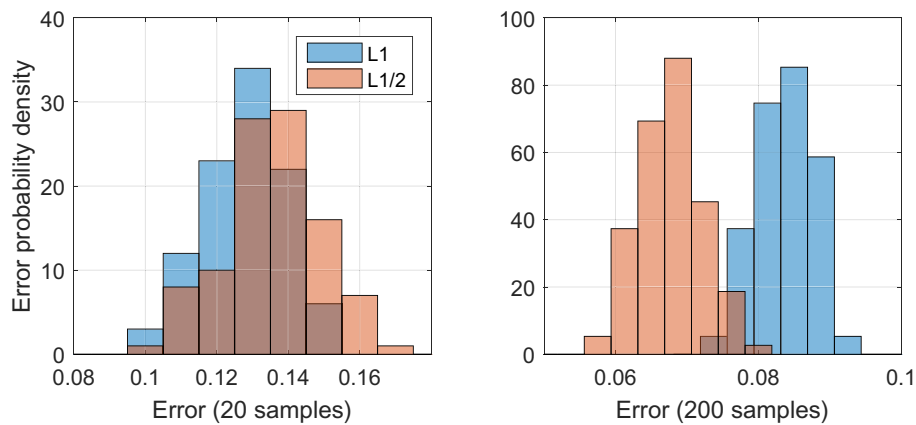

Fig. 18. Distribution of error over 100 repeated estimations of Eq. (46) with re-weighting for 20 and 200 samples.

als are shown (Fig. 18) providing greater insight into the reconstruction effectiveness. The results here are similar to those for the re-weighted stationary case. In particular, L_1 norm minimization is superior at lower sample numbers, with $L_{1/2}$ norm improving at a higher rate with increasing sample numbers. Again for 200 samples, the $L_{1/2}$ norm solution appears to be always superior.

6. Concluding remarks

In this paper, a general L_p norm ($0 < p \leq 1$) minimization approach has been proposed for estimating stochastic process power spectra subject to realizations with missing data. In particular, focusing on the L_1 and $L_{1/2}$ norms, it has been shown that the approach can be significantly enhanced by an adaptive basis re-weighting scheme, while it can satisfactorily estimate the power spectra of stationary, non-stationary, and multi-dimensional processes, even in cases of 80% missing data.

Also, it has been shown that there are clear advantages to utilizing $L_{1/2}$ norm over L_1 norm minimization in signal reconstruction for power spectrum estimation. In particular, when dealing with single process records for which the presented adaptive basis re-weighting procedure cannot be applied, $L_{1/2}$ norm minimization exhibits superior performance to L_1 norm. In addition, where multiple realizations are available for basis re-weighting, $L_{1/2}$ norm is shown to provide more accurate spectrum estimations when large sample sizes are utilized. Nevertheless, differences in the effect of re-weighting have been observed. Although the improvement in spectrum estimation accuracy was significant for both $L_{1/2}$ and L_1 norm minimization when utilizing the re-weighting procedure, L_1 norm minimization has been shown to exhibit a greater magnitude of improvement after re-weighting when compared to $L_{1/2}$. This is due to the fact that the re-weighting procedure has a sparsity-enhancing effect, which leaves less room for an $L_{1/2}$ solution to exhibit greater sparsity than an L_1 solution. Nevertheless, despite the re-weighting, the $L_{1/2}$ solution still succeeds in producing sparser spectral estimates. For a signal that is not truly sparse, such as those considered in this paper, this additional sparsity can be an advantage or disadvantage depending on the number of samples available. For large sample sizes, the $L_{1/2}$ norm minimization has produced superior results

across all of the examples. However, in the stationary and the two-dimensional cases, for small sample sizes the opposite has been true. Thus, for small sample numbers in particular, when dealing with reconstruction of processes for which limited information regarding their degree of sparsity is available, estimates from both minimization schemes should be utilized within a decision-making process.

Acknowledgement

References

[1] R.A. Muller, G.J. MacDonald, Ice Ages and Astronomical Causes: Data, Spectral Analysis and Mechanisms, second ed., Praxis Publishing, Chichester, UK, 2002.
[2] N. Lomb, Least-squares frequency-analysis of unequally spaced data, Astrophys. Space Sci. 39 (2) (1976) 447–462.
[3] J. Scargle, Studies in astronomical time-series analysis. 2. Statistical aspects of spectral-analysis of unevenly spaced data, Astrophys. J. 263 (2) (1982) 835–853.
[4] P. Vanicek, Approximate spectral analysis by least-squares fit – successive spectral analysis, Astrophys. Space Sci. 4 (4) (1969) 387.
[5] J.A. Högbom, Aperture synthesis with a non-regular distribution of interferometer baselines, Astron. Astrophys. Supp 15 (1974) 417 provided by the SAO/NASA Astrophysics Data System.
[6] S. Baisch, G. Bokelmann, Spectral analysis with incomplete time series: an example from seismology, Comput. Geosci. 25 (7) (1999) 739–750.
[7] D. Roberts, J. Lehar, J. Dreher, Time-series analysis with clean. 1. Derivation of a spectrum, Astron. J. 93 (4) (1987) 968–989.
[8] G. Fahlman, T. Ulrych, A new method for estimating the power spectrum of gapped data, Mon. Not. R. Astron. Soc. 199 (1) (1982) 53–65.
[9] E.J. Candès, J. Romberg, T. Tao, Robust uncertainty principles: exact signal reconstruction from highly incomplete frequency information, IEEE Trans. Inf. Theory 52 (2) (2006) 489–509.
[10] D.L. Donoho, Compressed sensing, IEEE Trans. Inf. Theory 52 (4) (2006) 1289–1306.
[11] Y. Yang, S. Nagarajaiah, Output-only modal identification by compressed sensing: non-uniform low-rate random sampling, Mech. Syst. Signal Process. 56 (2015) 15–34.
[12] Z. Zou, Y. Bao, H. Li, B.F. Spencer, J. Ou, Embedding compressive sensing-based data loss recovery algorithm into wireless smart sensors for structural health monitoring, IEEE Sens. J. 15 (2) (2015) 797–808.
[13] D. Mascarenas, A. Cattaneo, J. Theiler, C. Farrar, Compressed sensing techniques for detecting damage in structures, Struct. Health Monit. (2013), 1475921713486164.
[14] Y. Wang, H. Hao, Damage identification scheme based on compressive sensing, J. Comput. Civil Eng. 29 (2) (2013) 04014037.
[15] A. Perelli, L. De Marchi, L. Flamigni, A. Marzani, G. Masetti, Best basis compressive sensing of guided waves in structural health monitoring, Digit. Signal Process. 42 (2015) 35–42.
[16] R.M. Levine, J.E. Michaels, S.J. Lee, D.O. Thompson, D.E. Chimenti, Guided wave localization of damage via sparse reconstruction, AIP Conference Proceedings-American Institute of Physics, vol. 1430, 2012, p. 647.
[17] S.M. O'Connor, J.P. Lynch, A.C. Gilbert, Implementation of a compressive sampling scheme for wireless sensors to achieve energy efficiency in a structural health monitoring system, in: SPIE Smart Structures and Materials+Nondestructive Evaluation and Health Monitoring, International Society for Optics and Photonics, 2013, pp. 86941L–86941L.
[18] M. Haile, A. Ghoshal, Application of compressed sensing in full-field structural health monitoring, in: SPIE Smart Structures and Materials +Nondestructive Evaluation and Health Monitoring, International Society for Optics and Photonics, 2012, pp. 834618–834618.
[19] J.B. Harley, A.C. Schmidt, J.M. Moura, Accurate sparse recovery of guided wave characteristics for structural health monitoring, in: 2012 IEEE International Ultrasonics Symposium, IEEE, 2012, pp. 158–161.
[20] Y. Bao, H. Li, X. Sun, Y. Yu, J. Ou, Compressive sampling–based data loss recovery for wireless sensor networks used in civil structural health monitoring, Struct. Health Monit. 12 (1) (2013) 78–95.
[21] R. Klis, E.N. Chatzi, Vibration monitoring via spectro-temporal compressive sensing for wireless sensor networks, Struct. Infrastruct. Eng. 13 (1) (2017) 195–209.
[22] L. Comerford, I.A. Kougioumtzoglou, M. Beer, Compressive sensing based stochastic process power spectrum estimation subject to missing data, Probab. Eng. Mech. 44 (2016) 66–76.
[23] M. Shinozuka, G. Deodatis, Simulation of stochastic processes by spectral representation, Appl. Mech. Rev. 44 (4) (1991) 191–204.
[24] J. Chen, J. Li, Optimal determination of frequencies in the spectral representation of stochastic processes, Comput. Mech. 51 (5) (2013) 791–806.
[25] J. Chen, W. Sun, J. Li, J. Xu, Stochastic harmonic function representation of stochastic processes, J. Appl. Mech. 80 (1) (2013) 011001.
[26] L. Comerford, M. Beer, I. Kougioumtzoglou, et al, Compressive sensing based power spectrum estimation from incomplete records by utilizing an adaptive basis, in: 2014 IEEE Symposium on Computational Intelligence for Engineering Solutions (CIES), IEEE, 2014, pp. 117–124.
[27] L. Comerford, H. Jensen, F. Mayorga, M. Beer, I. Kougioumtzoglou, Compressive sensing with an adaptive wavelet basis for structural system response and reliability analysis under missing data, Comput. Struct. 182 (2017) 26–40.
[28] E.J. Candes, M.B. Wakin, S.P. Boyd, Enhancing sparsity by reweighted l1 minimization, J. Fourier Anal. Appl. 14 (5–6) (2008) 877–905.
[29] Y. Huang, J.L. Beck, S. Wu, H. Li, Robust bayesian compressive sensing for signals in structural health monitoring, Comput.-Aided Civil Infrastruct. Eng. 29 (3) (2014) 160–179.
[30] Y. Huang, J.L. Beck, S. Wu, H. Li, Bayesian compressive sensing for approximately sparse signals and application to structural health monitoring signals for data loss recovery, Probab. Eng. Mech. 46 (2016) 62–79.
[31] M.A. Davenport, M.F. Duarte, Y.C. Eldar, G. Kutyniok, Introduction to Compressed Sensing, Compressed Sensing: Theory and Applications, Cambridge University Press, 2012.
[32] R. Chartrand, Exact reconstruction of sparse signals via nonconvex minimization, IEEE Signal Process. Lett. 14 (10) (2007) 707–710.
[33] A. Bandeira, E. Dobriban, D. Mixon, W. Sawin, Certifying the restricted isometry property is hard, IEEE Trans. Inf. Theory 59 (6) (2013) 3448–3450.
[34] V.M. Patel, R. Chellappa, Sparse Representations and Compressive Sensing for Imaging and Vision, Springer Science & Business Media, 2013.
[35] I. Orovic et al, Multimedia Signals and Systems, Springer Science & Business Media, 2012.
[36] R. Chartrand, V. Staneva, Restricted isometry properties and nonconvex compressive sensing, Inverse Prob. 24 (3) (2008) 035020.
[37] Z. Xu, H. Zhang, Y. Wang, X. Chang, Y. Liang, L1/2 regularization, Sci. China Inf. Sci. 53 (6) (2010) 1159–1169.
[38] I.F. Gorodnitsky, B.D. Rao, Sparse signal reconstruction from limited data using focuss: a re-weighted minimum norm algorithm, IEEE Trans. Signal Process. 45 (3) (1997) 600–616.
[39] R. Chartrand, W. Yin, Iteratively reweighted algorithms for compressive sensing, in: 2008 IEEE International Conference on Acoustics, Speech and Signal Processing, IEEE, 2008, pp. 3869–3872.
[40] D.E. Newland, An Introduction to Random Vibrations, Spectral and Wavelet Analysis, third ed., Longmans Scientific & Technical, Harlow, 1993.

[41] M. Priestley, Evolutionary spectra and non-stationary processes, J. Roy. Stat. Soc. Ser. B-Stat. Methodol. 27 (2) (1965) 204–237.
[42] J. Liang, S.R. Chaudhuri, M. Shinozuka, Simulation of nonstationary stochastic processes by spectral representation, J. Eng. Mech.-ASCE 133 (6) (2007) 616–627.
[43] G.P. Nason, R. von Sachs, G. Kroisandt, Wavelet processes and adaptive estimation of the evolutionary wavelet spectrum, J. Roy. Stat. Soc. Ser. B (Stat. Methodol.) 62 (2) (2000) 271–292.
[44] R. Dahlhaus, Fitting time series models to nonstationary processes, Ann. Stat. 25 (1) (1997) 1–37.
[45] D.E. Newland, An Introduction to Random Vibrations, Spectral & Wavelet Analysis, Courier Corporation, 2012.
[46] D.E. Newland, Harmonic and musical wavelets, Proc. Roy. Soc. London Ser. A-Math. Phys. Eng. Sci. 444 (1922) (1994) 605–620.
[47] P.D. Spanos, I.A. Kougioumtzoglou, Harmonic wavelets based statistical linearization for response evolutionary power spectrum determination, Probab. Eng. Mech. 27 (1) (2012) 57–68.
[48] P. Spanos, J. Tezcan, P. Tratskas, Stochastic processes evolutionary spectrum estimation via harmonic wavelets, Comput. Meth. Appl. Mech. Eng. 194 (12–16) (2005) 1367–1383.
[49] P.D. Spanos, G. Failla, Evolutionary spectra estimation using wavelets, J. Eng. Mech.-ASCE 130 (8) (2004) 952–960, pT: J; TC: 16; UT: WOS:000223001200010.
[50] I.A. Kougioumtzoglou, F. Kong, P.D. Spanos, J. Li, Some observations on wavelets based evolutionary power spectrum estimation, Proceedings of the Stochastic Mechanics Conference (SM12), Ustica, Italy, vol. 3, 2012, pp. 37–44, ISSN: 2035–679X.
[51] K. Hasselmann, T. Barnett, E. Bouws, H. Carlson, D. Cartwright, K. Enke, J. Ewing, H. Gienapp, D. Hasselmann, P. Kruseman, et al, Measurements of wind-wave growth and swell decay during the joint north sea wave project (jonswap). Tech. rep., Deutches Hydrographisches Institut, 1973.
[52] X. Chen, Analysis of alongwind tall building response to transient nonstationary winds, J. Struct. Eng. 134 (5) (2008) 782–791.
[53] K. Teferra, S.R. Arwade, G. Deodatis, Generalized variability response functions for two-dimensional elasticity problems, Comput. Meth. Appl. Mech. Eng. 272 (2014) 121–137.
[54] M. Shinozuka, G. Deodatis, Simulation of multi-dimensional gaussian stochastic fields by spectral representation, Appl. Mech. Rev. 49 (1) (1996) 29–53.
[55] M. Grigoriu, Applied Non-Gaussian Processes: Examples, Theory, Simulation, Linear Random Vibration, and MATLAB Solutions, Prentice Hall, 1995.
[56] P. Bocchini, G. Deodatis, Critical review and latest developments of a class of simulation algorithms for strongly non-gaussian random fields, Probab. Eng. Mech. 23 (4) (2008) 393–407.
[57] M. Shields, G. Deodatis, P. Bocchini, A simple and efficient methodology to approximate a general non-gaussian stationary stochastic process by a translation process, Probab. Eng. Mech. 26 (4) (2011) 511–519.
[58] G. Deodatis, R.C. Micaletti, Simulation of highly skewed non-gaussian stochastic processes, J. Eng. Mech. 127 (12) (2001) 1284–1295.